eXPRESS Polymer Letters Vol.1, No.3 (2007) 150–156
Available online at www.expresspolymlett.com
DOI: 10.3144/expresspolymlett.2007.24

Synthesis, characterizations and electro-optical properties of nonlinear optical polyimide/silica hybrid

F. X. Qiu[1*], *P. P. Li*[2], *D. Y. Yang*[1]

[1]School of Chemistry and Chemical Engineering, Jiangsu University, Zhenjiang 212013, China
[2]Jiangsu Provincial Key Laboratory of Modern Agricultural Equipment and Technology, Zhenjiang 212013, China

Received 17 November 2006; accepted in revised form 27 February 2007

Abstract. Transparent Nonlinear Optical (NLO) inorganic/organic (polyimide/silica) hybrid composites with covalent links between the inorganic and the organic networks were prepared by the sol-gel method. The silica content in the hybrid films was varied from 0 to 22.5/wt%. The prepared PI hybrids were characterized by IR, UV-Vis, Thermogravimetric analysis (TGA), X-ray diffraction (XRD), Scanning Electron Microscopy (SEM) and Transmission Electron Microscopy (TEM). They exhibited fair good optical transparency. The SiO_2 phase was well dispersed in the polymer matrix. DSC and TGA results showed that these hybrid materials had excellent thermal stability. The polymer solutions could be spin coated on the indium-tin-oxide (ITO) glass to form optical quality thin films. The electro-optic coefficients (γ_{33}) at the wavelength of 832 nm for polymer thin films poled were in the range of 19–27 pm/V.

Keywords: *polymer composites, nonlinear optical, hybrid, electro-optical property*

1. Introduction

Organic polymeric second-order nonlinear optical (NLO) materials have been extensively studied due to their potential application in integrated photonic devices such as high-speed electro-optic (EO) modulators and switches optical data storage and information processing [1–3]. It is most remarkable that recent improvements in various polyimide systems have resulted in several waveguide devices based on the second-order NLO polymers. However, to develop practical devices, the challenge of achieving excellent tradeoffs in all the properties of the NLO polymers (i.e. EO coefficients, thermal, chemical, and photochemical stability, temporal dipole alignment stability, optical loss, dielectric constant and mechanical properties) still exists [4–6]. However, inorganic glasses are excellent photonic media because of their high optical quality, extremely low optical losses and thermal stability. Therefore, combining inorganic glass and organic photo-functional molecules is probably one of the best ways of getting optical waveguide materials with large optical nonlinearity and low losses.

Combining organic polymers with inorganic oxides using variations of the sol-gel method has become prevalent for the past 10 years as a means of preparing organic-inorganic hybrid and inorganic glasses [7–10]. The preparation of the films with high transmission coefficient from infrared to about 220 nm by sol-gel method was considered a successful technique since this way, high quality waveguide devices were obtained intended to applications in integrated optics for telecommunications [11–12]. On the other hand, the sol-gel processes with low processing temperature allows the incorporation of organic polymer networks leading to the formation of organic-inorganic hybrid materials.

*Corresponding author, e-mail: fxqiuchem@163.com

In this study, we synthesized an electro-optical chromophore (Figure 1), hydroxyl polyimide based on the fluorine-containing monomers, 6FDA-6FHP (Figure 2) and side-chain NLO polyimide 6FDA-6FHP-NLO (Figure 3). We report the sol-gel synthesis of organic-inorganic silica waveguide materials (Figure 4), and investigated the optical properties, thermal properties and micrographs study.

2. Experimental

2.1. Materials and characterization

N, N-dimethylacetamide (DMAc) were stirred over powered calcium hydride overnight and then distilled under reduced pressure and stored over 4 Å molecular sieves. The 4,4'-(Hexafluoroisopropylidene) diphthalic Anhydride (6FDA) and 2,2-Bis (3-amino-4-hydroxyphenyl) hexafluoropropane (6FHP) used in the polyimide synthesis were obtained from TCI and used without further purification. The 3-aminopropyltriethoxysilane, APTES was purchased from Nanjing shuguang chemical plant. Tetrahydrofuran (THF) was purified by distillation and other reagents and solvents were obtained commercially and were used as received.

IR spectra of the prepared thin films were obtained on a KBr pellet using Nicolet AVATAR 360 spectrometer. To examine the optical characteristics of materials with addition of sample light transmission was measured in ultraviolet and visible range by means of a spectrophotometer (Shimadzu UV-240). The fracture surfaces of hybrid thin films were examined on a HITACHI X-650 Scanning Electron Microscope (SEM). HITACHI H-600 Transmission Electron Microscope (TEM) measured the particle sizes. Thermogravimetric analysis (TGA) and differential scanning calorimetry (DSC) were performed on NETZSCH STA449C. The programmed heating range was from room temperature to 800°C, at a heating rate of 10°C/min under a nitrogen atmosphere. The measurement was taken using 6–10 mg samples. TGA and DSC curves were recorded. X-ray diffraction (XRD) patterns of SiO_2 were obtained with a CuKα X-ray source and a step of 0.02(2θ) and run from 2θ = 6~80° at room temperature. The elemental analysis was determined on the Foss Heraeus CHN-O-Rapid.

2.2. Synthesis of a NLO chromophore

To a stirred solution of p-nitroaniline (13.8 g, 0.10 mol) in methanol/HCl (50%, V/V, 50 ml) was added sodium nitrite (6.90 g, 0.10 mol) in ice-water (15%, m/m) at 0°C [13–16]. The mixture was stirred at this temperature for 1 h. Meanwhile stirred solution of aminobenzene purified by distillation (9.3 g, 0.10 mol) in HCl (50 ml, 1 mol·l^{-1}). Then these two solutions were mixed and sodium nitrite (6.90 g, 0.10 mol) was added in ice-water (15%, m/m) at 0°C. The mixture was added dropwise into a solution of N-2-hydroxyethyl-N-methylaniline (15.10 g, 0.10 mol) with excess HAc-NaAc. The mixture was stirred at 40–50°C for 20 min. The mixture solution was cooled down and placed for 2 h, and the solid was collected by filtration and further recrystallized from toluene/methanol (4:1) to give a bright red crystal. ^{1}H NMR (300 MHz, acetone-d_6, ppm): 10.61 (s, OH, 1H), 8.05 (s, ArH, 2H), 8.00 (s, ArH, 2H), 7.83 (s, ArH,

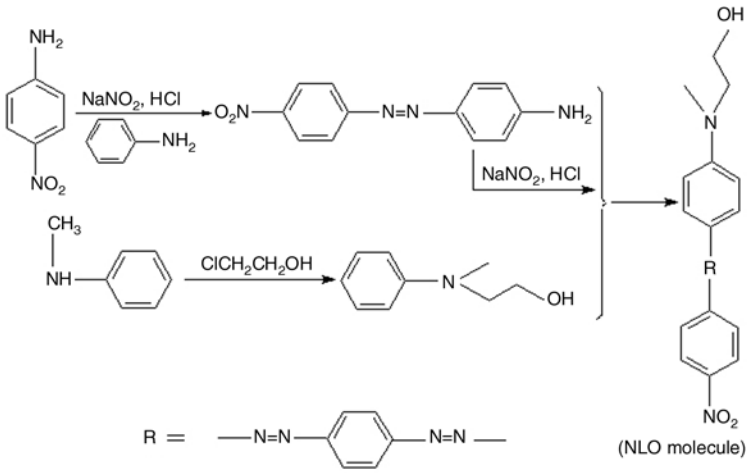

Figure 1. Synthesis of the NLO chromophore molecule

2H), 7.11 (s, ArH, 2H), 6.56 (s, ArH, 2H), 6.20 (s, ArH, 2H), 4.20 (s, $–CH_2CH_2O–$, 2H), 3.73 (s, $–CH_2CH_2O–$, 2H), 2.46 (s, $–CH_3$, 3H). Anal. Calcd for $C_{21}H_{20}N_6O_2$: C, 62.38%; H, 4.95%; N, 20.79%. Found: C, 62.48%; H, 4.89%; N, 20.82%. The synthetic route is shown in Figure 1.

2.3. Hydroxyl polyimide synthesis

The polymerization was conducted in a dry nitrogen flushed three-neck flask with a magnetic stirrer, reverse Dean-stark trap, and reflux condenser filled dry xylene. A stoichiometric amount of 6FDA (3.33 g, 7.5 mmol) was added to a solution of 6FHP (2.7 5g, 7.5 mmol) in 30 ml DMAC at 0°C. The solution was then warmed to room temperature and magnetically stirred overnight under nitrogen to form the poly (amic acid) solution. Dry xylene (30 ml) was added to the flask, and the poly (amic acid) was thermally cyclized in an oil bath at 160°C for 5 h under nitrogen atmosphere. The resulting solution was added dropwise into a solution of methanol/water (1:1, V/V, 50 ml) and 2NHCl (10 ml) in a high-speed blender to obtain the polyimide A or B. The product was filtered and washed with methanol/water (1:1, 10 ml) three times, and dried at 60°C under vacuum for 24 h. **A** ^{1}H NMR (300 MHz, CD_3COCD_3, ppm): 10.65 (s, OH, 2H), 8.44 (s, ArH, 2H), 8.35 (d, ArH, 2H), 8.33 (s, ArH, 2H), 7.62 (s, ArH, 2H), 7.32 (d, ArH, 2H), 7.10 (d, ArH, 2H). Anal. Calcd for $C_{34}H_{14}F_{12}N_2O_6$: C, 52.71%; H, 1.81%; N, 3.62%. Found: C, 52.79%; H, 1.78%; N, 3.66%. The molecular weight was measured by GPC and has Mn of 17,800, M_w of 37,300 with a polydispersity of 2.10 (polystyrenes as standards). The synthetic route was shown in Figure 2.

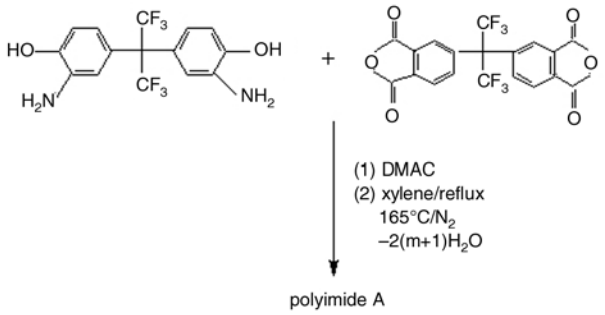

Figure 2. Synthetic route for hydroxyl polyimide

2.4. Synthesis of side-chain NLO polyimide

The polyimide A (0.39 g, 0.5 mmol), PPh_3 (0.39 g, 1.5 mmol) and 4-(N-2-hydro-xyethyl-N-methyl-anino)-4'-(p-nitrobenzene-diazenyl) azobenzene (NLO chromophere) (0.40 g, 1.00 mmol) were dissolved in THF (15 ml). Diethyl azodicarboxylate (DEAD) (0.26 g, 1.50 mmol) was added dropwise into the solution under nitrogen atmosphere. The reaction mixture was stirred for 2 days at room temperature, and then the resulting reaction solution was added dropwise into an agitated solution of methanol/water (1:1,30 ml) and 2N HCl (5 ml) in a high-speed blender. The collected solid further precipitated in THF (10 ml) and reprecipitated into the solution of methanol/water. The product was filtered out and washed with methanol/water for several times, and dried at 60°C under vacuum for 24 h. **B** ^{1}H NMR (300 MHz, CD_3COCD_3, ppm): 8.46 (s, ArH, 2H), 8.38 (d, ArH, 2H), 8.35 (s, ArH, 2H), 8.06 (s, ArH, 4H), 7.99 (s, ArH, 4H), 7.85 (s, ArH, 4H), 7.63 (s, ArH, 2H), 7.33 (d, ArH, 2H), 7.13 (d, ArH, 2H), 7.08 (s, ArH, 4H), 6.55 (s, ArH, 4H), 6.21 (s, ArH, 4H), 4.19 (s, $–CH_2CH_2O–$, 4H), 3.66 (s, $–CH_2CH_2O–$, 4H), 2.40 (s, $–CH_3$, 6H) Anal. Calcd for $C_{76}H_{50}F_{12}N_4O_{10}$: C, 59.00%; H, 3.23%; N, 12.68%. Found: C, 59.06%; H, 3.21%; N, 12.73%. The molecular weight was measured by GPC and has an M_n of 19,600, an M_w of 41,400 with a polydispersity of 2.11 (polystyrenes as standards). The synthetic route is shown in Figure 3.

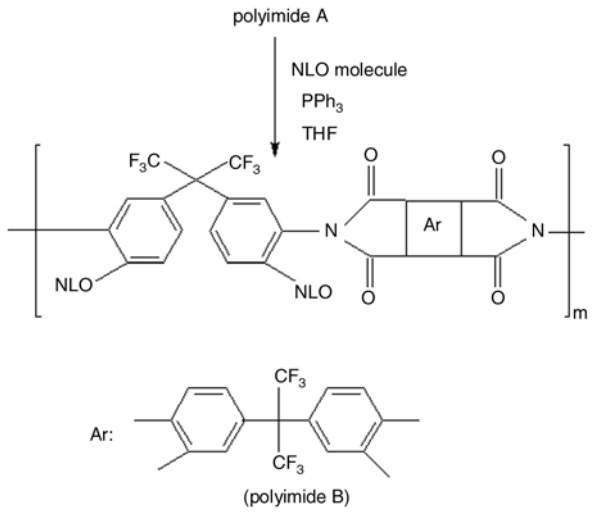

Figure 3. Synthetic route for side-chain NLO polyimide

2.5. Synthesis of inorganic-organic hybrid waveguide materials

Hybrid materials were successfully synthesized via sol-gel process. Its technique is based on creating two individual homogeneous inorganic and organic solutions, which are then mixed together and allowed to react at room temperature with carefully controlled evaporation conditions. The first homogeneous inorganic solution is a partially acid hydrolyzed alkoxide sol in THF, while the second homogenous organic solution is an APTES functionalized polyimide in THF. Furthermore, the presence of the pendant APTES groups on the functionalized polyimide facilitates chemical bonding with the partially hydrolyzed alkoxide sol via condensation reactions as shown in Figure 1. At the completion of the evaporation step of the previously mixed inorganic and organic solutions, further heat treatments are used to promote additional conversion of the alkoxide xerogel domains via condensation reactions. The hybrid material was prepared by systematically varying the concentration of the tetrathylorthosilicate (TEOS). The silicon alkoxide content is reported as a weight percent in the hybrid system and is based on the loading mass and not on the mass of silica after the sol-gel process. This is shown in Figure 4. Table 1 summarized the various hybrid systems fabricated for this study.

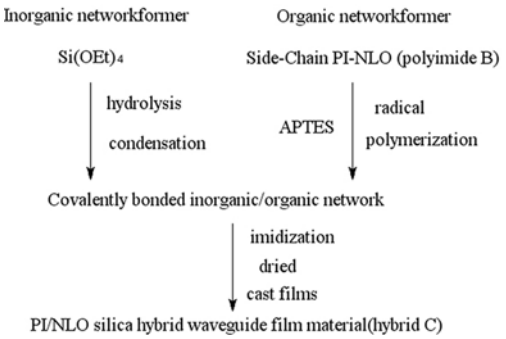

Figure 4. Synthesis of polyimide/silica hybrid waveguide systems

3. Results and discussion

Figure 5 illustrates the FT-IR spectra of the prepared polyimide-silica hybrid thin films C-1, C-2, C-3 and C-4. The characteristic absorption bands of the imide group are observed at 730, 1378, 1716, 1776 cm^{-1} for all samples. The intensity of the absorption band around 1000~1140 cm^{-1} gradually increases with increasing silica content, consistent with the formation of the three-dimensional Si–O–Si network in the hybrid film [17–18]. The broad absorption around 3100~3500 cm^{-1} are assigned to the Si–OH residue, formed in the hydrolysis of alkoxy groups of TEOS. This band is barely detectable in the spectrum of C-1 with lower silica content but increases its intensity in that of C-4 with higher silica content [19]. Besides, the FT-IR spectrum consists of some peaks located at 1520 cm^{-1} (ν_{as}, –N=N–), 1364 cm^{-1} (ν_{str}, –C–N–C–), 1345 cm^{-1} (ν_{s}, $–NO_2$), 1378 cm–1 (wagging CH_2), 695 cm^{-1} (wagging N–H), indicating that the silica xerogel networks is composed of Si–O–Si backbones and some organic groups.

Figure 6 and Figure 7 present the SEM and TEM micrographs of the prepared polyimide-silica hybrid thin films C-2 and C-4. In most cases, surface morphology of materials is of great impor-

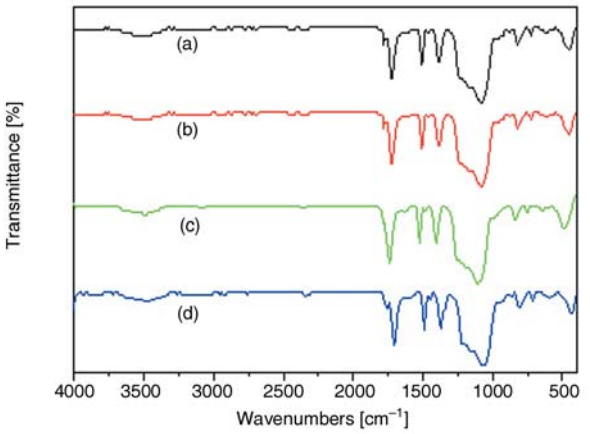

Figure 5. FT-IR spectrums of C-1 (a), C-2 (b), C-3 (c) and C-4 (d)

Table 1. Reactant Summary and properties of polyimide and hybrid systems

Materials	TEOS [wt%]	polyimide [g]	APTES [ml]	HCl [ml]	H_2O [ml]	THF [ml]	Appearance[a] [ml]	T_g[b] [°C]	T_d[c] [°C]	γ_{33} [pm/V]
C	0							225	340	27
C-1	5	2.55	0.20	0.10	0.25	30	Transparent	348	459	25
C-2	10	2.55	0.20	0.25	0.53	30	Transparent	353	462	23
C-3	15	2.55	0.20	0.50	1.02	30	Transparent	356	469	20
C-4	22.5	2.55	0.20	0.65	2.10	30	Transparent	362	472	19

[a]UV-Vis spectrum was observed; [b]Experimental results from DSC; [c]Experimental results from TGA

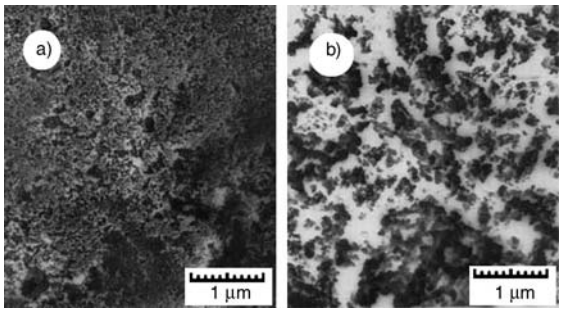

Figure 6. SEM photographs of C-2 (a) and C-4 (b)

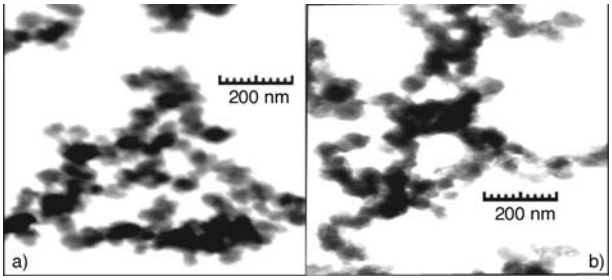

Figure 7. TEM photographs of C-2 (a) and C-4 (b)

tance for many technical applications requiring well-defined surfaces or interfaces. The SEM figures reveal that no phase separation. That is, the covalent bonding (Si–O–Si) between the organic and inorganic components enhanced miscibility. Both components were homogeneously and uniformly dispersed at a molecular level. When the silica content was below 15 wt%, the silica particle size was 50 nm, as indicated in Figure 7. However, when the silica content was increased to 22.5 wt%, the particle size was increased to 80 nm. The increase in the silica particle size clearly resulted from the increase in the aggregation tendency as the silica content and the silica particle number were increased. These micrographs show the fine interconnected or co-continuous phases morphology, which improve the efficiency of stress transfer mechanisms between the two components.

XRD measurements were inferred by estimating the crystallizability of the hybrid material (C-2). From Figure 8, the diffractogram typical of amorphous samples can be seen, The XRD pattern of the hybrid films (C-3) display only a very broad hump centered at $2\theta = 23.55°$; originating from amorphous phase of aromatic polyimide. This result also indicates that covalent bonding (Si–O–Si) between the organic and inorganic components enhanced miscibility.

To examine thermal activities of hybrid materials in higher temperature range and their thermal decomposition characteristics, DSC and TGA

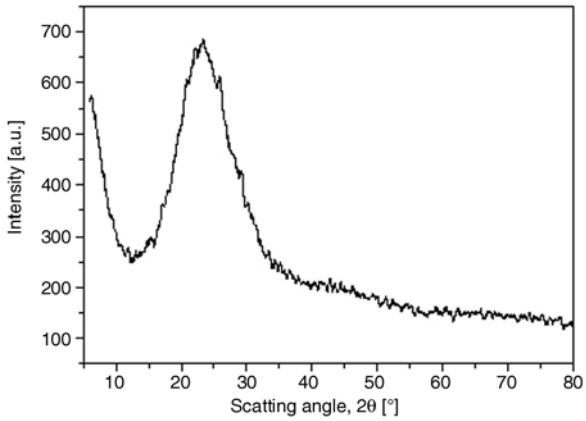

Figure 8. XRD patterens of the C-3

experiments were carried out on NETZSCH STA449C with the heating rate 10°C/min under nitrogen. Their data listed in Table 1. Compared with the pure *E* or *F*, the initial degradation temperature (T_d) of hybrid materials increased with the increase of TEOS moiety. The enhanced thermal stability of hybrid materials is due to the formation of network of polyimide and the inorganic moieties, which results from the restriction of polymer chain mobility and becomes more intertwined with the rigid silica network. Therefore, the existence of covalent bonds between polyimide and silica impose even more restraints to chain movement in hybrids. DSC analysis shows glass transition temperature (T_g) for the polyimide- silica network in the hybrids at 348~362°C. Based on what was mentioned the above, the compatibility of the PI/SiO_2 hybrid can be enhanced via incorporating polymer matrix with inorganic silica covalently. The chemical bonding not only restricts the migration of inorganic silicates but also hinders the aggregation of silanol [20]. It is estimated that these materials will be pretty good for the practical application.

High-quality films could be easily prepared from the polyimides and hybrids solutions in NMP by spin coating on ITO glass. The electro-optic (EO) coefficient measurement of our nanohybrid was performed at a wavelength of 832 nm. The test sample consisted of a high-index prism, a thin silver film, a poled material layer, a buffer layer, and a base silver film. The silver film was thermally evaporated onto the hypotenuse face of a high-index prism as the first electrode. The thickness of the film was about 55 nm. A polymer was spin coated onto the silver substrate to a thickness of 1–2 µm, which can support four or five surface-plasmon modes with TE or TM polarization. A

polymer buffer layer was then coated onto the polyimide film to a thickness of 3–5 μm or so. Corona discharge poling was performed by alignment of the chromophore dipoles in a high static electric field while the polyimide was heated to high mobility close to its glass transition temperature. The poling voltage was 1500 V. Finally; another silver film was deposited onto the buffer layer as the second electrode. The γ_{33} values were listed in Table 1. From the Table 1, the γ_{33} coefficients of hybrids were smaller than corresponding polyimide. This was due to the content of chromophore is smaller than the pure polyimide. Therefore, these results showed that these polymers might be useful in photonic device applications.

4. Conclusions

Transparent Nonlinear Optical (NLO) inorganic/organic waveguide films systems had been prepared in situ sol-gel process. They have network structure and silica particles were uniformly dispersed on the nanoscale. Covalent bonding (Si–O–Si) between the organic and inorganic components enhanced miscibility between the silica and the copolymer. The thermogravimetric analysis and differential scanning calorimetry behavior indicate excellent thermal stability. The resulting polyimide/silica hybrids exhibited a relatively high $T_g > 348$°C and thermal stability up to 448°C. Large EO coefficient values (20–30 pm/V) at the wavelength of 832 nm were achieved and the values remained well.

Acknowledgements

This work was financially supported by the Jiangsu Planned Projects for Postdoctoral Research Funds (0602037B), the Natural Science of Jiangsu Education (05KJB150016) and the fund of Jiangsu University (06JDG015).

References

[1] Dalton L. R., Harper A. W., Ghosn R., Steier W. H., Ziari M., Fetterman H., Shi Y., Mustacich R. V., Jen A. K. Y., Shea K. J.: Synthesis and processing of improved organic second-order nonlinear optical materials for applications in photonics. Chemistry of Materials, **7**, 1060–1081(1995).

[2] Burland D. M., Miller R. D., Walsh C. A.: Second-order nonlinearity in poled-polymer systems. Chemical Reviews, **94**, 31–75 (1994).

[3] Marder S. R., Kippelen B., Jen A. K-Y., Peyghamarian N.: Design and synthesis of chromophores and polymers for electro-optic and photorefrative applications. Nature, **388**, 845–851(1997).

[4] Leng W. N., Zhou Y. M., Xu Q. H., Liu J. Z.: Synthesis and characterization of nonlinear optical side – Chain polyimides containing the benzothiazole chromophores. Macromolecules, **34**, 4774–4779 (2001).

[5] Qiu F. X., Zhou Y. M., Liu J. Z., Zhang X. P.: Preparation, morphological and thermal stability of polyimide/silica hybrid material containing dye NBDPA. Dyes and Pigments, **71**, 37–42 (2006).

[6] Watanabe O., Tsuchimori M., Okada A., Ito H.: Electro-optic intensity modulator using a vovel urethane-urea copolymer. Japanese Journal of Applied Physics, **37**, 5588–5592 (1998).

[7] Loy D. A., Shea K. J.: Bridged polysilsesquioxanes. Highly porous hybrid organic-inorganic materials. Chemical Reviews, **95**, 1431–1442 (1995).

[8] Wen J. Y., Wilkes G. L.: Organic/inorganic hybrid network materials by the sol-gel approach. Chemistry of Materials, **8**, 1667–1681 (1996).

[9] Chung C. M., Lee S. J., Kim J. G., Jang D. O.: Organic-inorganic polymer hybrids based on unsaturated polyester. Journal of Non-Crystalline Solids, **311**, 195–198 (2002).

[10] Kim J. H., Lee Y. M.: Gas permeation properties of poly(amide-6-b-ethylene oxide)-silica hybrid membranes. Journal of Membrane Science, **193**, 209–225 (2001).

[11] Najafi S. I., Touam T., Sara R., Andrews M. P., Fardad M. A.: Sol-gel glass waveguide and grating on silicon. Journal of Lightwave Technology, **16**, 1640–1646 (1998).

[12] Alvarez-Santos S., Gonzalez-Lafont A., Lluch J. M.: On the intramolecular proton transfers in N,N'-bis(salicydene)-p-phenylene diamine. New Journal of Chemistry, **18**, 873–877 (1994).

[13] Qiu F. X., Jiag Y., Zhou Y. M., Liu J. H.: Synthesis, characterization and thermal properties of novel PMDA-PAPD/silica hybrid network polymers. Silicon Chemistry, **3**, 65–73 (2006).

[14] Qiu F. X., Zhou Y. M., Liu J. Z.: The synthesis and characteristic study of 6FDA-6FHP-NLO polyimide/SiO_2 nanohybrid materials. European Polymer Journal, **40**, 713–720 (2004).

[15] Saadeh H., Gharavi A., Yu D., Yu L. P.: Polyimides with a diazo chromophore exhibiting high thermal stability and large electrooptic coefficients. Macromolecules, **30**, 5403–5407 (1997).

[16] Cojocariu C., Rochon P.: Thermotropic side-chain liquid crystalline copolymers containing both mono- and bisazobenzene mesogens: synthesis and properties. Macromolecules, **38**, 9526–9538 (2005).

[17] Que W. X., Hu X.: Sol-gel derived titania/γ-glycidoxypropyltrimethoxysilane and methyltri methoxysilane hybrid materials for optical waveguides. Journal

of Sol-Gel Science and Technology, **28**, 319–325 (2003).

[18] Cornelius C. J., Marand E.: Hybrid inorganic-organic materials based on a 6FDA- 6FpDA-DABA polyimide and silica: physical characterization studies. Polymer, **43**, 2385–2400 (2002).

[19] Zheng M. P., Gu M. Y., Jin Y. P., Jin G. L.: Preparation, structure and properties of TiO_2-PVP hybrid films. Materials Science and Engineering: B, Solid State Materials for Advanced Technology, **77**, 55–59 (2000).

[20] Hsiue G. H., Kuo W. J., Huang Y. P., Jeng R. J.: Microstructural and morphological characteristics of PS-SiO_2 nanocomposites. Polymer, **41**, 2813–2825 (2000).